D/13

N84 15603

DYNAMIC CERTIFICATION OF A THRUST-MEASURING SYSTEM FOR LARGE SOLID ROCKET MOTORS*

R. A. LeMaster and R. B. Runyan
Sverdrup Technology, Inc./AEDC Group

INTRODUCTION

The J-4 Rocket Test Cell and its Thrust Measuring System (TMS) at Arnold Engineering Development Center (AEDC) were modified to provide multicomponent force measurement of large solid rocket motors having nozzle gimbaling capability. To verify the structural integrity of a combined TMS and motor system, a large finite element model of the TMS and motor was developed using the MSC/NASTRAN computer program. Due to the importance of obtaining accurate estimates for the dynamic force levels, it was necessary to certify that the model adequately simulated the physical system. This was accomplished by performing a modal analysis test on the TMS and motor combination. The objectives of this paper are: (1) to discuss the physical characteristics of the TMS and motor that influence the MSC/NASTRAN model; (2) to compare the frequency response characteristics computed using the MSC/NASTRAN model to those obtained from the modal analysis test; (3) to discuss the experiences gained in modal analysis testing; and (4) to demonstrate how state-of-the-art experimental and analytical methods are used in the design of ground test facilities.

Due to economic and/or time constraints associated with performing experimental investigations on large, complex structures, the structural analyst rarely has the opportunity to determine how well his finite element representation simulates the characteristics of the actual structure. Finite element calculations have been shown to agree very well with experimental data for simple components. However, little data is available concerning how well they agree for complex structures comprised of many components. Since the TMS and motor combination are comprised of structural components from aerospace, mechanical, and civil engineering disciplines, the methods, results, comparisons, and conclusions drawn from this activity will be of interest to the dynamics and structures community in general.

In the following sections, descriptions of the TMS, finite element model, and modeling assumptions will be given in conjunction with the analysis methods. Subsequent sections will discuss the experimental effort and compare the experimental data to the computed results.

---

*The work reported herein was performed by the Arnold Engineering Development Center (AEDC), Air Force Systems Command (AFSC). Work and analysis for this research were done by personnel of Sverdrup Technology, Inc., operating contractor of the AEDC Engine Test Facility. Further reproduction is authorized to satisfy the needs of the U. S. Government.

THRUST-MEASURING SYSTEM

During simulated altitude testing, the motor is restrained by a large fixture which is referred to as the Thrust-Measuring System. The TMS is designed to react and measure the six components of thrust developed by the motor, and is rated at 2.2 MN (500,000 lb) axial force and 222.2 kN (50,000 lb) side force. The TMS is very massive, using eight W 36 x 400 beams to react the primary forces. The location of the TMS within the J-4 Rocket Test Cell is shown in figure 1. Figure 2 shows the main thrust stand structure prior to installation in the test cell.

During testing, the TMS is required to withstand large dynamic forces created by ignition and gimbaling transients. The magnitude of the dynamic forces may be several times the static values and is a function of the motor dynamics and its interaction with the TMS.

The TMS contains a large number of structural connections, many of which contain secondary members which intersect with primary members at odd angles. In general, the depth of the secondary members is significantly less than that of the primary member, and the secondary members are welded only to the flange or web of the frame member. Consequently, the mechanical behavior of the connections is quite complex. Three typical connections are shown in figures 3a, b, and c.

Figure 3a shows one of eight connections where the main thrust-measuring system structure connects to a 3.048-m (10 ft) support column. The support column is made from 0.91-m (36 in.)-diameter thick-walled pipe and has longitudinal stiffeners located every 36 deg around its circumference. As seen in figure 3a, several secondary support and bracing members attach to the main girder and intersect it at odd angles at various locations (i.e., flange or web). Since the secondary member intersecting the main girder web is much smaller than the main girder, the plate behavior of the main girder web will influence the stiffness of the connection.

Figure 3b shows another connection used several times in the TMS. Again, note the relative size of the main girder and secondary member; the plate behavior of the web will influence the connection stiffness characteristics. Also shown in figure 3b is a typical triaxial strain gage accelerometer and mounting block installation. The orientation and positioning of the accelerometers and mounting blocks are discussed in a subsequent section.

Figure 3c shows another typical connection in which the secondary members intersect the main girder at odd angles, and are much smaller than the main girder. Clearly, the load-deflection behavior of these connections will be quite complex.

FINITE ELEMENT ANALYSIS

Experience has shown that significant dynamic interactions may develop during ignition and gimbaling transients. The magnitudes of the dynamic interactions are influenced by coupling between the vertical and lateral motion of the TMS as it responds to the load transients. Therefore, it is necessary that the complicated modes of vibration characterizing the TMS be adequately defined.

A large finite element model of the TMS and motor combination was developed using the MSC/NASTRAN computer program. The finite element model of the TMS (shown graphically in figure 4) is comprised primarily of beam elements. Truss elements were used to represent the load-measuring column behavior; the flexures were treated as pinned connections. Experimentally obtained axial stiffness coefficients for the load-measuring columns were used to establish the equivalent properties of the truss elements.

The magnitude of the effort required to model the connections using three-dimensional continuum or plate elements dictated that assumptions be made regarding the kinematic behavior of the connections. It was often necessary to idealize a connection as being either fixed or pinned; in some cases linear constraint equations were written to describe the kinematic behavior of the connections. This type of connection idealization is universally used in the day-to-day application of finite element programs to the analysis of frame structures; it is also one of the more significant approximations. In later sections, the impact of the connection modeling assumptions will be discussed in light of the accuracy of the computed modes.

Mass and stiffness matrices of the solid rocket motor were obtained from the motor manufacturer and added to the structural model of the TMS. The case of the motor was represented using shell elements, and the propellant was represented by three-dimensional, continuum-type elements. A simplified material representation of the propellant was used which represented its anticipated frequency response characteristics. However, the viscous character of the propellant was not considered.

The motor and TMS models were combined using standard substructuring methods (references 1 and 2). Since the two models were developed by two different companies, it was not possible to use the automated substructuring techniques available in the MSC/NASTRAN computer program. Therefore, the partitioning and merging matrix operations necessary to combine the two models were implemented through direct matrix abstraction program (DMAP) modifications to the appropriate rigid format solution modules. The partitioning vectors for both the motor and TMS matrices were supplied as input in the bulk data decks. The mass and stiffness matrices representing the motor were transmitted to and from permanent disc storage using the INPUT4 and OUTPUT4 IO modules.

The combined TMS and motor model was used to compute the first thirty natural frequencies and mode shapes of the system. The system response to various excitation sources was obtained through superposition of the modal responses. To make the analysis more manageable, the integration of the uncoupled equations and the subsequent summation of the modal responses were performed outside of NASTRAN, using in-house software as illustrated in figure 5. Using this technique, stresses were obtained in an interactive manner on an element-by-element basis. When it was determined that the stress history in a particular element was required, the stress-displacement matrix for that element was created using the geometric and material data from the NASTRAN bulk data deck. The appropriate modal displacements were subsequently determined using the eigenvalues and time histories of the generalized coordinates; the appropriate stresses were then computed. This technique proved to be very efficient and significantly decreased the amount of peripheral storage required to retain the dynamic stress and displacement histories. The only quantities saved were the time histories of the generalized coordinates and the mode shapes, or eigenvectors. It was also very convenient since the analyst did not have to specify which displacements and stresses he wished to have printed out or retained prior to executing the actual analysis (as required by many finite element programs). This method also significantly reduced royalty costs associated with using MSC/NASTRAN, since NASTRAN was used only to assemble the component matrices and compute the natural frequencies and mode shapes; all remaining computations were performed outside of NASTRAN.

EXPERIMENTAL MODAL SURVEY

In recent years an impact testing technique commonly referred to as "modal analysis testing" has been developed which enables the natural frequencies and modal properties of a system to be determined experimentally. In addition, the mode shapes may be displayed in animated motion on a graphics computer terminal. The modal analysis methods enable the structural analyst to study a particular mode of the structure and to compare the frequency and mode shape to those obtained from a finite element analysis. In addition, the damping associated with a particular mode can be obtained and used as input to the finite element model. One benefit of the modal analysis method is that it provides experimental data in a form directly compatible with the results of a finite element analysis. The analyst may then evaluate which modes are accurately represented, and may gain insight as to how the finite element model may be improved.

Modal testing requires both the excitation and the response of the structure to be recorded. The excitation and response time histories are transformed to the frequency domain, and the frequency response function relating the response to the excitation is obtained. The selective acquisition of a family of frequency response functions having a common excitation point enables the modal parameters of the structure to be obtained. For detailed treatments on modal analysis methods, the interested reader is referred to references 2 through 10.

To adequately define the complicated mode shapes of the TMS and the motor combination, three-dimensional accelerometer readings were required at 54 different locations on the structure. This resulted in having accelerometer response data at almost every major connection on the structure (figure 6). An actual motor having an inert propellant was used to insure that the dynamic characteristics of the motor were properly represented.

The quality of the modal analysis results is directly proportional to the quality of the excitation and response time history data. A major problem at the onset of the modal analysis effort was to determine how to excite the structure to such an extent that the low-frequency response (1-30 Hz) of the structure could be measured. It is a relatively easy matter to excite the high-frequency modes of a structure, but to adequately excite the low-frequency modes of massive structures is not as simple. In addition, a time constraint required that the modal testing be completed within a short time, including instrumentation and hardware setup.

Impact Method No. 1

Two different instrumentation and impact device configurations were tried. The basic idea behind the first setup was to obtain accelerometer response data at as many locations as possible for each impact. The advantage of this approach is that it enabled the experimental data to be obtained quickly. A major disadvantage is that every channel of the data cannot easily be visually inspected on an oscilloscope as the data are being recorded. Therefore, it is not known until the data are being reduced whether all channels contain good data.

Accelerometers available for this test were in the 5- and 10-G range and were of the strain gage type. Computations performed using the finite element representation of the structure indicated that a 400-kN (90,000 lb) impact force would be required to excite the low-frequency modes sufficiently to obtain a good signal. A device designed to deliver the impact force, shown in figure 7, consisted of a pendulum having a swing radius of 3.048m (10 ft). The pendulum bob [a 10.16-cm (4 in.)-diam by 60.96-cm (24 in.)-long steel cylinder] was allowed to swing free and impact on the anvil containing a quartz force ring; it was manually caught on rebound to prevent multiple impacts. The pendulum impact device was designed to excite modes having a significant participation in the lateral direction.

Several problems were encountered which limited the usefulness of the pendulum impact device and associated instrumentation. These are listed below:

1. The impact device did not yield clean impulse time domain profiles and corresponding frequency spectra. Discontinuities in the impact anvil and force ring assembly resulted in partial reflection of the impact force, and the "hammer" chattered with the anvil surface during contact. Details of the anvil assembly are shown in figure 8.

2. Instrumentation problems prevented obtaining good data on all recorder channels for a given impact.

3. The accelerometers were not sensitive enough to obtain good signal-to-noise ratio signals.

Impact Method No. 2

To overcome the problems encountered with the high energy impact setup, a commercially available instrumented sledge hammer and a high sensitivity seismic accelerometer, shown in figure 9, were used. The sledge hammer is capable of developing up to a 22-kN (5,000 lb) impact load, and provided a flat impulse spectrum over the frequency range of interest. The seismic accelerometer has a rated sensitivity down to 10^{-6} G, and weighs approximately one-half kilogram (one pound). Response data obtained using this hardware were on the order of 10^{-3} G. Compared to the first impact device, the instrumented sledge hammer provided a relatively low level energy input into the system.

The data were obtained using a roving accelerometer procedure in which a single accelerometer was moved to the various response locations; the impact location was considered the reference point throughout the modal analysis. To obtain accelerometer response data in three orthogonal directions of each data location on the structure, it was necessary to install mounting blocks at each location. The mounting blocks were fabricated to provide a flat surface perpendicular to each of the three measurement directions. A typical mounting block is shown in figure 3b, with a triaxial accelerometer mounted on its top face.

Since only one single-axis high sensitivity accelerometer was available, it was necessary to relocate the accelerometer in each of the three measurement directions at each measurement location. This was the most time-consuming operation of the entire job. To ensure that all modes of the structure had been excited, three different impact points having different impact directions were utilized. All three impact points were located on the aft firing ring of the motor.

This method requires considerably more time than the previous method. However, since only one pair of response and impact time signals was being recorded simultaneously, it was possible to view both the input and response signals on an oscilloscope as they were being recorded. This made it possible to ensure that good data were obtained at each response location. This proved to be a very important feature.

COMPARISON OF EXPERIMENTAL AND ANALYTICAL RESULTS

A comparison of the computed and experimentally determined frequencies and mode shapes is shown in Table I. As seen in Table I, the frequencies and general shape of the modes agreed very well for most of the modes. An evaluation of the results of this comparison shows that the finite element model was capable of computing those modes which were associated with the load-measuring columns and motor combination. In addition, the shell-type modes of the motor were represented well. However, modes controlled by the accumulated flexibility of the large structural beam connections (4, 5, and 8 of Table I) were not in good agreement.

CONCLUSIONS

This investigation concludes that state-of-the-art structural analysis computer programs such as NASTRAN can be used to successfully represent the dynamic characteristics of large thrust-measuring systems. The finite element model must include accurate representations of all major components comprising the system (i.e., thrust butt, load-measuring columns, motor, and propellant). However, it was also observed that the finite element models of frame structures which utilize kinematic constraints to represent complex connections may not represent all modes of the structure accurately. Fortunately, for the situation under consideration, the inaccurately represented modes did not contribute significantly to the response of the critical members.

The dynamic certification effort was considered successful since the experimental data indicated that the dominant modes expected to respond to the ignition and gimbaling transients were adequately represented by the combined finite element model of the motor and TMS.

The modal analysis results identified areas in the TMS which were "dynamically sensitive," and a careful review of the animated mode shapes suggested design changes which would improve the dynamic characteristics of the TMS.

The commercially available instrumented sledge hammer and seismic accelerometer combination provided the highest quality data, and enabled the data to be reviewed as it was being taken. The ability to inspect the data in the field proved to be very desirable when this type of experiment is performed. It was concluded that relatively low input force levels can be used to excite the low-frequency modes of massive structures by tuning the impact spectrum of the hammer.

The quality of the animated mode shape displays was adequate to determine the basic motion of the structure. However, in most cases one or more of the points in the animated display of the structure were in obvious error. In addition, it was difficult to discern exactly how the structure was deforming during some of the higher frequency modes.

Modal testing is a valuable tool for discerning the adequacy of a finite element representation, and can be successfully applied to very large structures used in ground test facilities.

REFERENCES

1. Przemieniecki, J. S.: Theory of Matrix Structural Analysis. McGraw-Hill, 1968.

2. Bathe, K. J. and Wilson, E. L.: Numerical Methods in Finite Element Analysis. Prentice-Hall, 1976.

3. Kennedy, C. C., and Pancu, C. D. P.: "Use of Vectors in Vibration Measurement and Analysis." Journal of the Aeronautical Sciences, Vol. 14, No. 11, November 1947, pp. 603-625.

4. Pendred, J. W. and Bishop, R. E. D.: "A Critical Introduction to Some Industrial Resonance Testing Techniques." Journal of Mechanical Engineering Science," Vol. 5, No. 4, 1963, pp. 345-367.

5. Klosterman, A. L.: "Determining Dynamic Information by Use of Vector Components of Vibration." M.S. Thesis in Mechanical Engineering, University of Cincinnati, 1968.

6. Klosterman, A. L.: "On the Experimental Determination and Use of Modal Representations of Dynamic Characteristics." Ph.D. Dissertation, University of Cincinnati, 1971.

7. Brown, D. L.: "Grinding Dynamics." Ph.D. Dissertation, University of Cincinnati, 1976.

8. Halversen, W. G. and Brown, D. L.: "Impulse Technique for Structural Frequencies Response Testing." Sound and Vibration, November 1977, pp. 8-21.

9. Tomlinson, G. R. and Hibbert, J. H.: "Identification of the Dynamic Characteristics of a Structure with Coulomb Friction." Journal of Sound and Vibration, Vol. 64, No. 2, 1979, pp. 233-242.

10. Goyder, H. G. D.: "Methods and Application of Structural Modeling from Measured Structural Frequency Response Data." Journal of Sound and Vibration, Vol. 68, No. 2, 1980, pp. 209-230.

ORIGINAL PAGE IS
OF POOR QUALITY

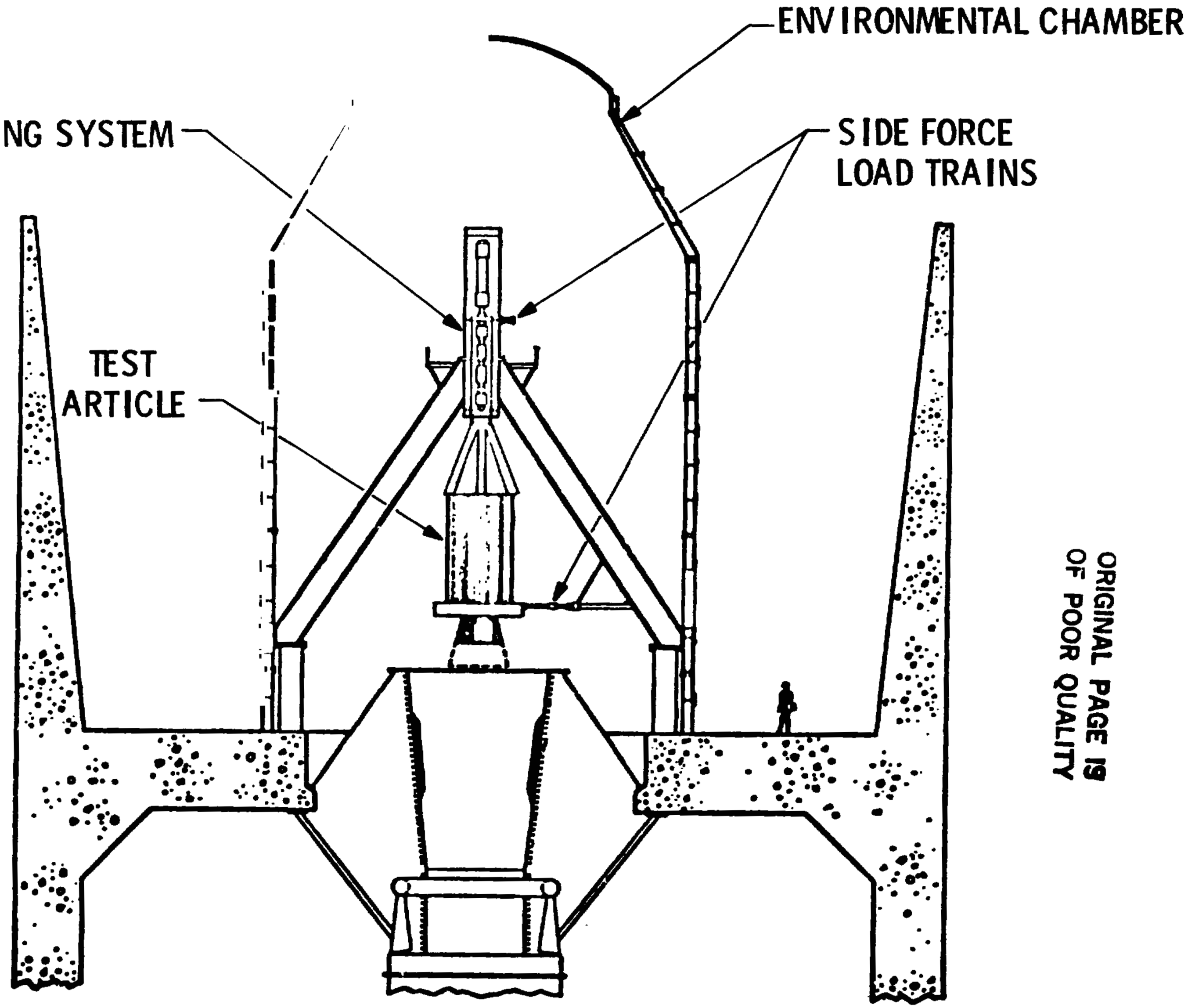

Figure 1. Thrust-Measuring System Installation

Figure 2. Thrust-Measuring System, Main Structure Pre-Installation

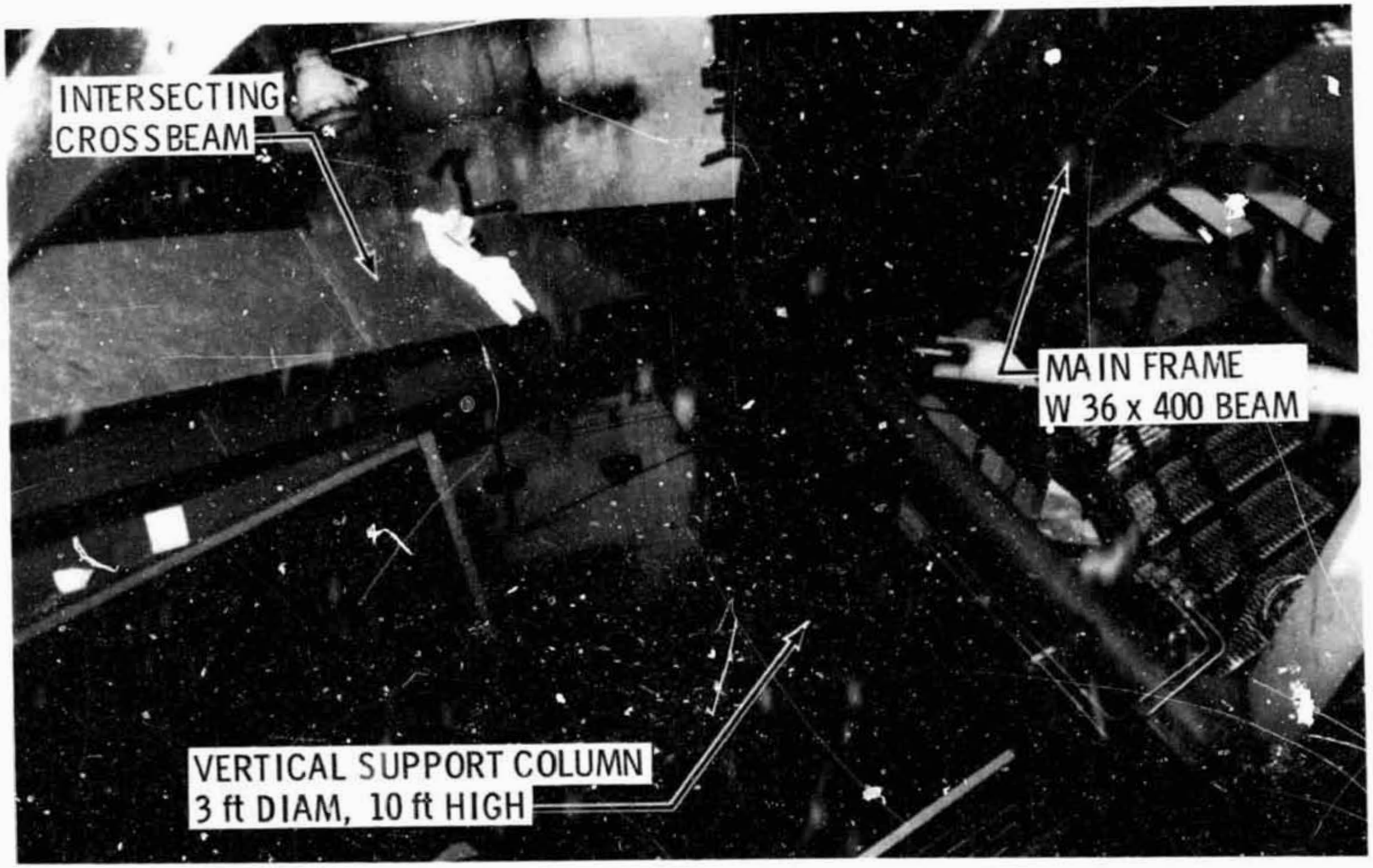

a. Lower frame connection

Figure 3. Details of Major Structural Connections

b. Mid frame 90-deg connection

Figure 3. Continued

ORIGINAL PAGE IS
OF POOR QUALITY

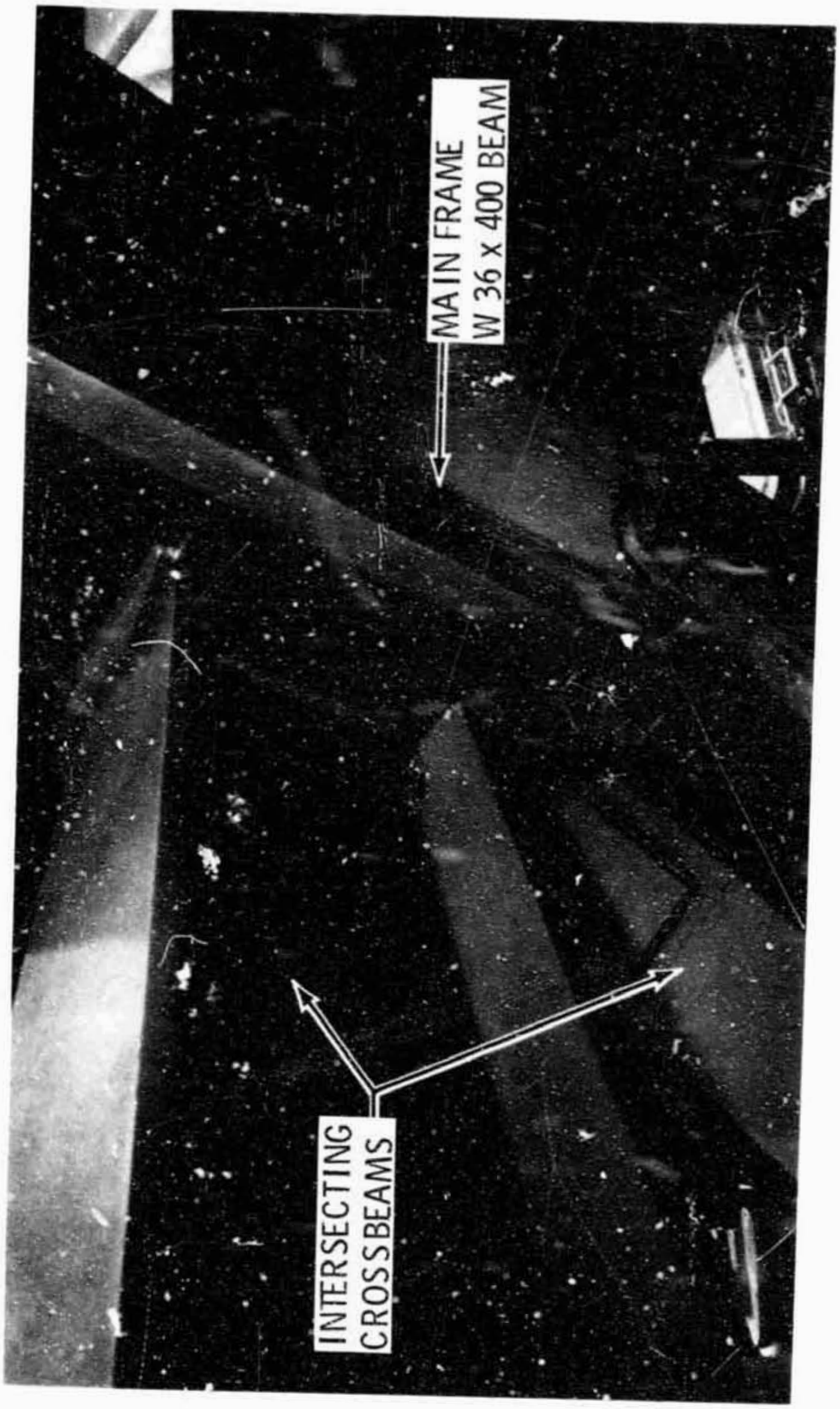

c. Mid frame double connection

Figure 3. Concluded

ORIGINAL PAGE IS
OF POOR QUALITY

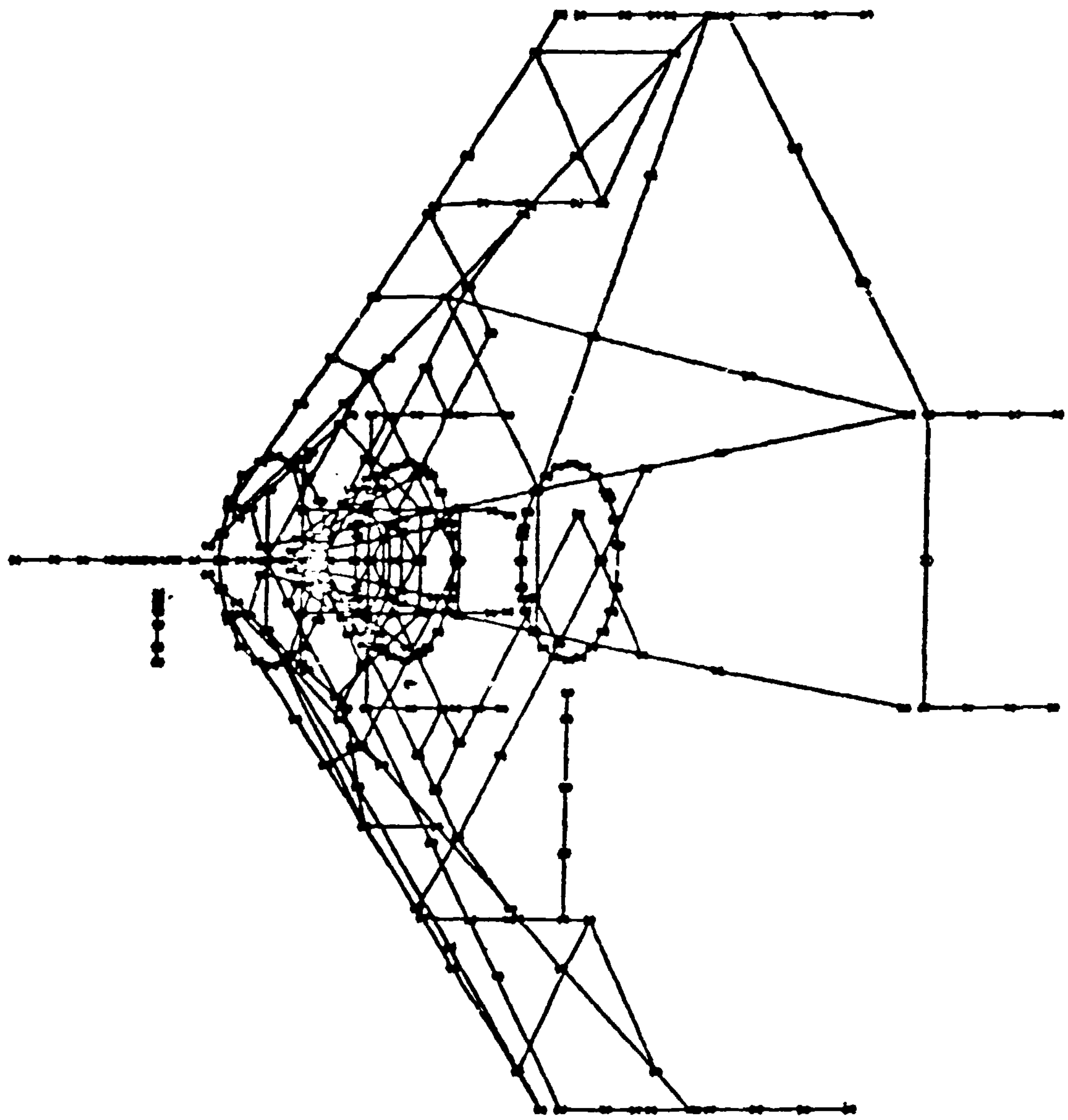

Figure 4. NASTRAN Finite Element Geometry Plot

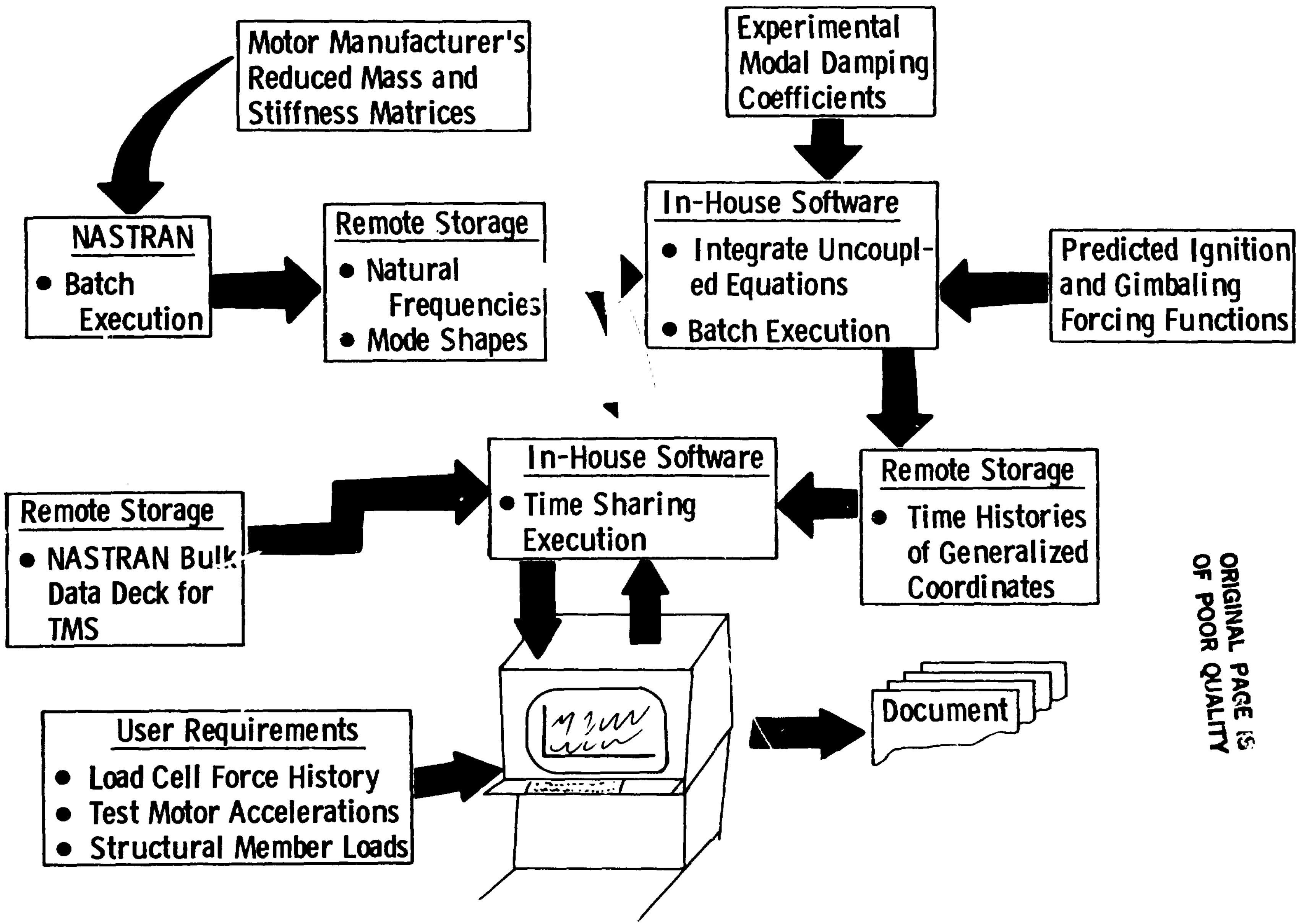

Figure 5. Flow of Information During Computational Study

ORIGINAL PAGE IS OF POOR QUALITY

ORIGINAL PAGE IS OF POOR QUALITY

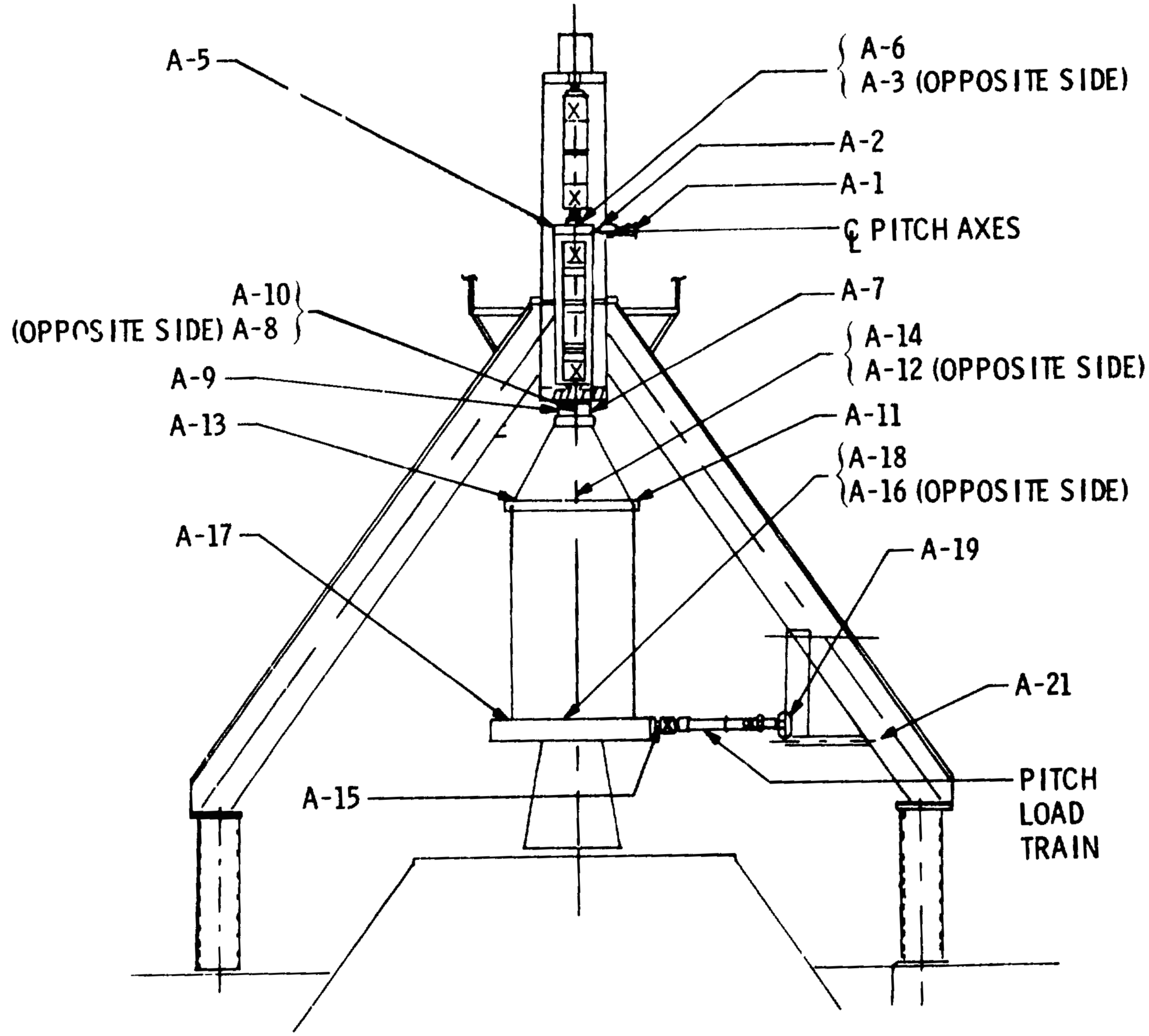

Figure 6. Accelerometer Locations, Elevation View, Pitch Plane

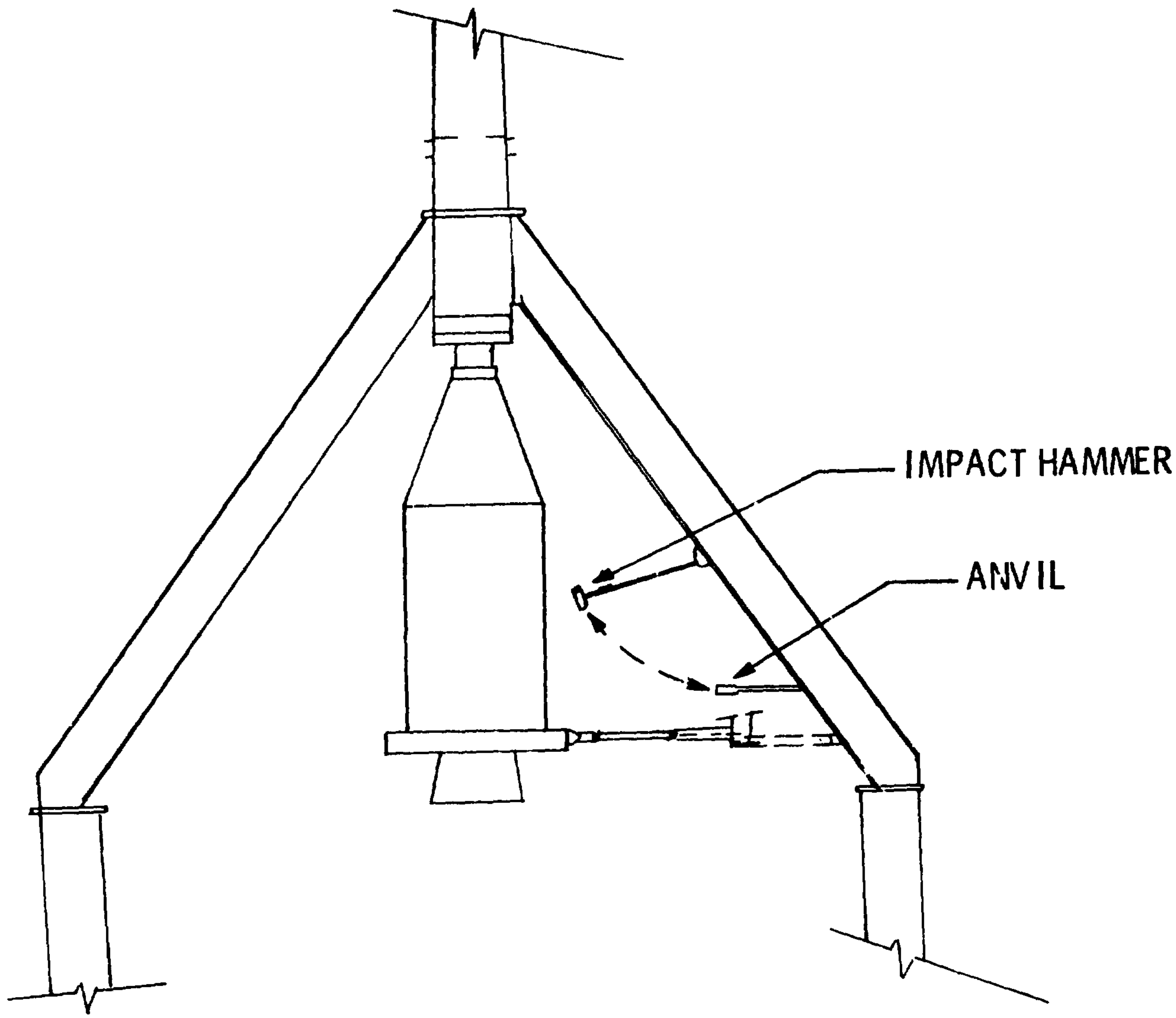

Figure 7. High Energy Impact Device Installation

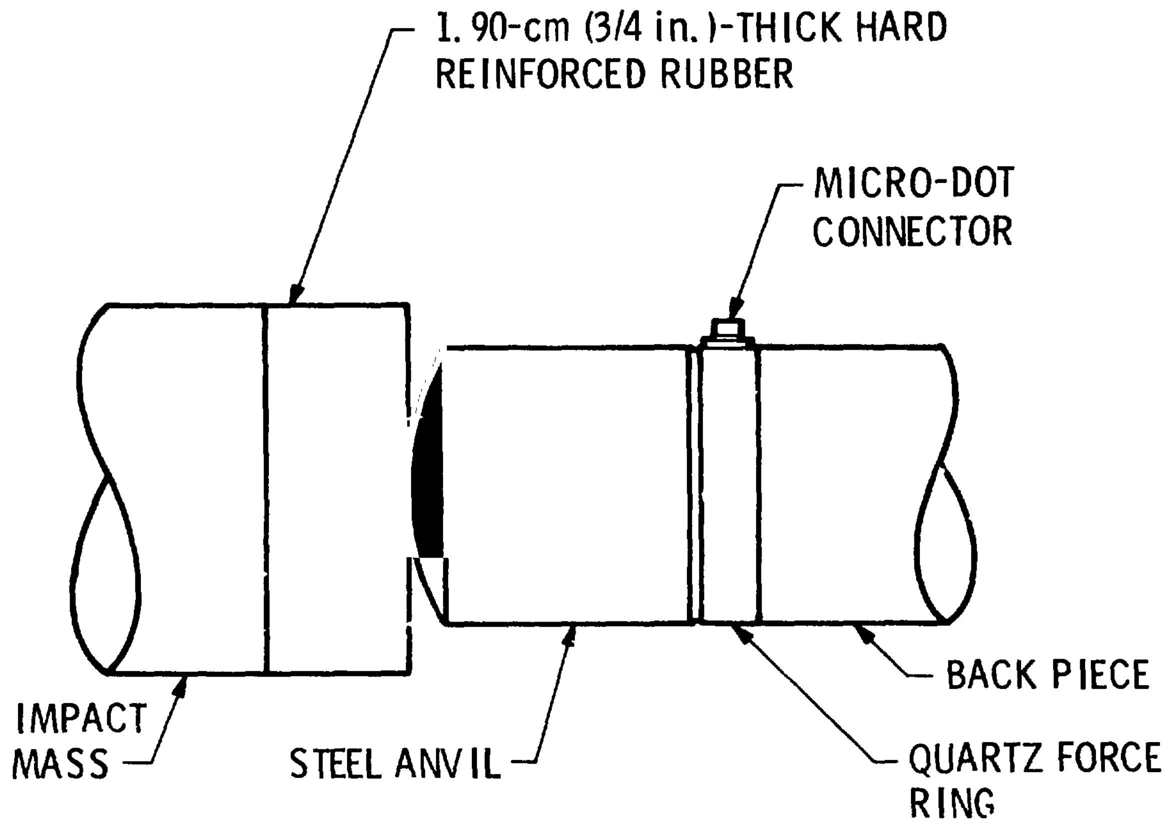

Figure 8. Impact Anvil Details

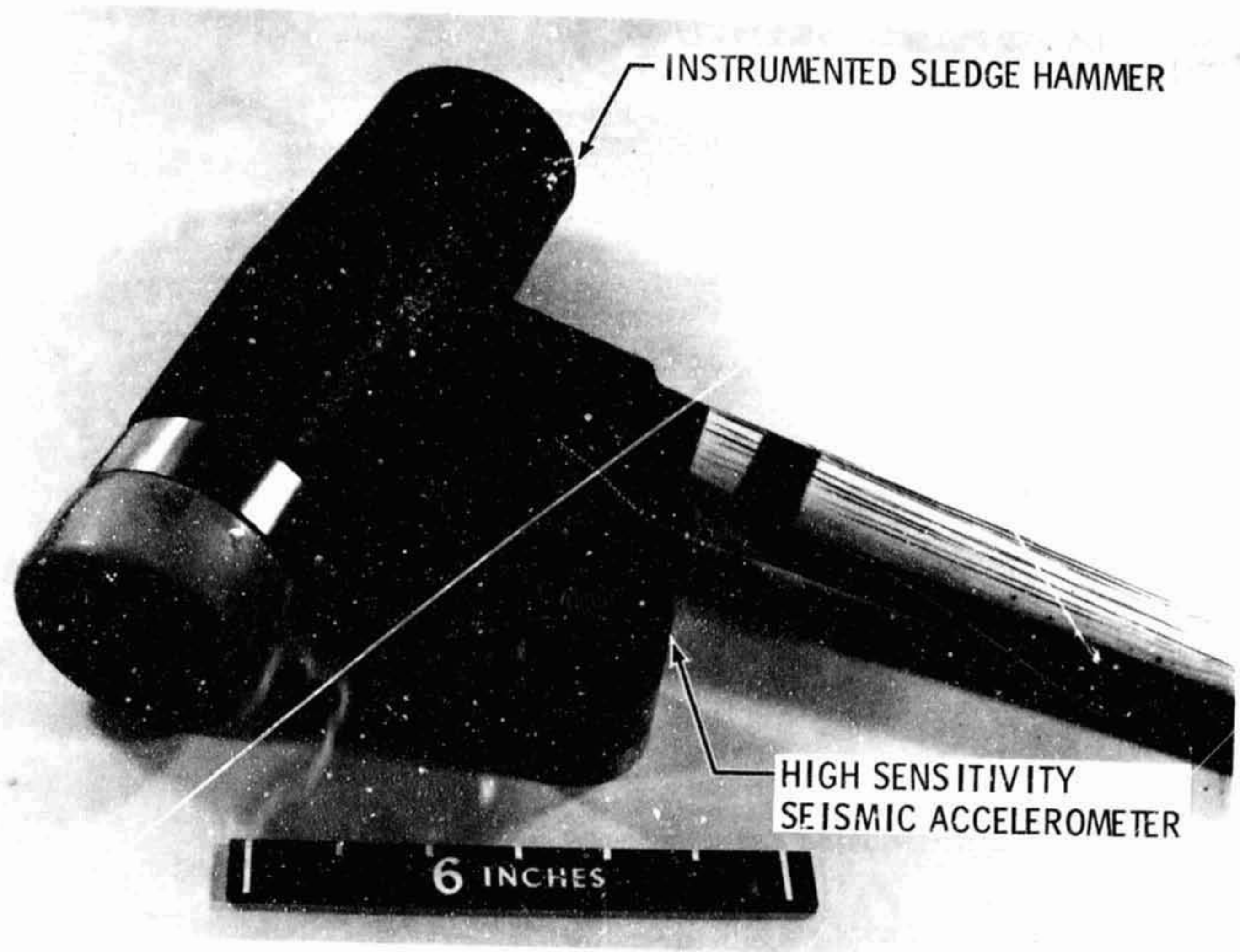

Figure 9. Impact and Measurement Devices

Table I. - Experimental and Computed Natural Frequencies

MODE NUMBER	EXPERIMENT (Hz)	COMPUTED (Hz)	DESCRIPTION OF MODE SHAPE
1	5.2	5.2	First lateral mode of motor in yaw direction.
2	5.6	5.6	First lateral mode of motor in pitch direction.
3	6.5	6.9	First rotational mode of motor.
4	7.5	*	Out-of-phase bending of inner thrust butt girders.
5	8.8	16.4	Breathing motion of thrust butt girders.
6	10.8	11.9	Vertical motion of motor on axial load column.
7	12.2	12.7	Second lateral mode of motor in yaw direction.
8	13.4	18.1	Out-of-phase bending of thrust butt main girders.
9	14.0	14.7	Second lateral mode of motor in pitch direction.
10	18.2	18.2	Lateral bending of X bracing and first bending mode of motor.

*Was not computed.